Shear-Stabilized Bi-axial Texture and Lamellar Contraction in both Diblock Copolymer and Diblock Copolymer/Homopolymer Blends

B. Scott Pinheiro,[†] Damian A. Hajduk,[‡,§] Sol M. Gruner,[‡] and Karen I. Winey*[,†]

Laboratory for Research on the Structure of Matter, Department of Materials Science and Engineering, University of Pennsylvania, Philadelphia, Pennsylvania 19104-6272, and Department of Physics, Princeton University, Princeton, New Jersey 08544-0708

Received August 29, 1995; Revised Manuscript Received December 8, 1995[⊗]

ABSTRACT: Large-amplitude oscillatory shear was applied to a poly(styrene-*b*-ethylenepropylene) diblock copolymer and also to binary blends of this copolymer with homopolystyrene. The shearing was applied at a temperature above the glass transition and well below the microphase separation transition for long times: 12 h, strain amplitude $\gamma = 40\%$, frequency $\omega = 1$ rad/s, $T = 150$ °C. The dynamic moduli decrease during the shearing and after a partial recovery upon annealing at 150 °C display a permanently altered rheological state. Small-angle X-ray scattering studies indicate that the shearing induces a biaxial texture consisting predominantly of a "parallel" orientation which coexists with a nearly "transverse" orientation of lamellae, inclined at ∼80° to the parallel orientation. The shearing also causes a ∼4% decrease in the lamellae spacing of the parallel orientation relative to the unsheared equilibrium state; lamellae in the nearly transverse orientation retain the equilibrium spacing. This lamellar contraction compares favorably to a recent theoretical treatment by Williams and MacKintosh [*Macromolecules* **1994**, *27*, 7677]. Upon annealing, the spacing of the lamellae in the parallel orientation expands to recover the equilibrium spacing, and the biaxial texture disappears via the loss of the nearly transverse orientation. After annealing, subjecting the sample to large-amplitude oscillatory shear a second time re-creates the biaxial texture.

I. Introduction

Block copolymer melts are of considerable interest because of their ability to self-assemble into ordered microdomains (lamellae, cylinders, etc.). These ordered nanostructures, which are periodic on the order of hundreds of angstroms, form domains or "grains" with dimensions typically on the order of microns. The effect of strong shear fields to macroscopically align these domains of microphase-separated block copolymers has received significant attention.[1−13]

Much of the research performed to date, including that presented here, has been on nearly symmetric lamellar diblock copolymer systems. Figure 1 displays a cartoon depicting three orthogonal orientations for lamellae relative to a shear field. In addition to the *parallel* and *perpendicular* orientations originally defined by Koppi et al., the *transverse* orientation[14] is defined as that having the lamellae oriented perpendicular to both the shearing surfaces and the shearing direction, that is the lamellar normal is aligned along the 1 direction. Researchers[5,7−9,15] have demonstrated that depending on the shearing conditions, either the parallel or the perpendicular orientation can be macroscopically induced. Also, under select circumstances, by altering the shearing conditions one of the orientations may be "flipped" to the other.

Principally two types of diblock copolymer systems have been studied, and the results obtained are not fully commensurate. The discrepancies may be due to the different molecular dynamics of the copolymer systems. In poly(ethylene propylene-*b*-ethylethylene) (PEP−PEE) copolymers[5,8,16,17] both blocks are well entangled but exhibit little mechanical contrast due to the similar glass transition temperatures of the blocks. In low molecular weight poly(styrene-*b*-diene) copolymers[6,7,9,15,18−20] there is significant mechanical contrast, but the styrene blocks have typically been below their entanglement molecular weight. We attempt to bridge the gap with the system studied here, poly(styrene-*b*-ethylenepropylene) (S−EP), which has both significant mechanical contrast and entanglement of both blocks.

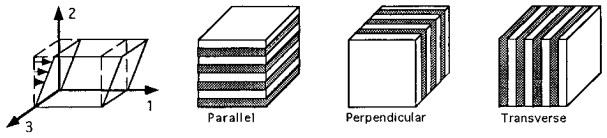

Figure 1. Coordinate system for the rheological and SAXS experiments showing three unidirectional orientations of lamellar block copolymers.

The initial goal of this research was to systematically alter the local molecular environment of the block copolymer chains by the addition of homopolymer to one of the microdomains. Changes in the molecular response of the system can be probed via the dynamic mechanical properties. Based on previous research,[21−23] we planned to maintain a lamellar morphology in our S−EP/S blends by appropriately selecting the molecular weight and concentration of the homopolystyrene and to create a globally aligned morphology by shearing.

While we obtained the lamellar morphology, our attempts to induce macroscopic alignment resulted in the creation of a shear stabilized biaxial texture which will be described in section IIIa. Section IIIb presents the mechanical response of the neat system as influenced by the strong shearing, and section IIIc presents the combined mechanical and morphological results for

* To whom correspondence should be addressed.
† University of Pennsylvania.
‡ Princeton University.
§ Current address: Department of Chemical Engineering and Material Science, University of Minnesota, Minneapolis, MN 55455.
⊗ Abstract published in *Advance ACS Abstracts,* February 1, 1996.

0024-9297/96/2229-1482$12.00/0

the blends. In the discussion, section IV, we describe the relationship between the rheological response and the state of macroscopic orientation in both the diblock copolymer and copolymer-rich diblock copolymer/homopolymer blends.[24] We also compare our experimentally observed shear-induced lamellar contraction to the theoretical prediction of Williams and MacKintosh.[25]

Recently, Okamoto et al.[26] reported *in situ* small-angle X-ray scattering (SAXS) results on an S−EP diblock copolymer (molecular weight of 130 000 and polystyrene volume fraction of 0.37) which is similar to ours. They show that applying large-amplitude oscillatory shear at different conditions can induce either a uniaxial parallel orientation of the lamellae or a biaxial texture, consisting of the parallel and transverse orientations, which is stable during shearing but unstable during quiescent annealing. Their SAXS findings for the biaxial texture agree substantially with ours and will also be discussed.

II. Experimental Section

Material. The lamellar poly(styrene-*b*-ethylenepropylene) diblock copolymer studied was Kraton G1701 provided by Shell Chemical Co. Size exclusion chromatography (SEC) was performed at the University of Pennsylvania using four Plgel 5 μm Mixed C columns in THF to measure a weight averaged molecular weight, M_w, of 110 000 relative to PS standards and a polydispersity, M_w/M_n, of 1.03. ^{1}H NMR was performed at the University of Pennsylvania in $CDCl_3$ with a 500 MHz field to measure a styrene monomer unit content of 28 mol %, which corresponds to 37 wt % PS. The material will therefore be referred to as SEP(40−70), corresponding to the nominal M_w's of the PS and PEP blocks. Using a Perkin-Elmer System 7 DSC at 20 °C/min, the glass transition temperature of the PS block was determined to be 102 °C. The microphase separation transition temperature, (MST) was not observed upon heating to ∼300 °C and has been estimated to be much greater than 300 °C,[26] making it experimentally inaccessible. The homopolystyrene, purchased from Pressure Chemical Co. (Pittsburgh, PA), was similarly characterized, revealing a glass transition temperature of 103 °C, $M_w \approx 30\,000$, and $M_w/M_n \approx 1.06$, and is designated as S(30).

Sample Preparation. A dilute solution (∼3 wt %) of the diblock copolymer (and homopolymer) in toluene was prepared with less than 1% Irgonox 1010 (Ciba-Geigy) added as an antioxidant. The solvent was slowly evaporated over 7−10 days to facilitate the development of equilibrium structures. The solution was well stirred by hand during the late stages of solvent evaporation in order to produce a more random orientation of the microphase-separated lamellar domains. The samples were then dried thoroughly in a vacuum oven at 40 °C for 24 h followed by 120 °C for ∼3 days. Samples for rheological testing were compression-molded in air at 150 °C and then annealed in a vacuum oven for 72 h at 150 °C. Blend samples are designated by the weight percent of homopolymer added.

Rheology. A Rheometrics Solids Analyzer (RSAII) (oscillatory shear, shear sandwich geometry, 1mm sample thickness) was used both to measure the dynamic mechanical properties of the samples and to induce macroscopic orientation in the samples. In order to obtain the rheological response of the sample without altering the response, a small shear amplitude was required. The rheological response was therefore characterized in the linear viscoelastic region by a *probe* condition of $\gamma = 1\%$, $\omega = 1$ rad/s, and 150 °C. In an attempt to induce macroscopic orientation, a large-amplitude oscillatory shear (LAOS), was applied at a temperature above the glass transition temperature and well below the MST. This orientation condition consisted of $\gamma = 40\%$, $\omega = 1$ rad/s, at 150 °C. The probe and orientation conditions are performed as time sweep experiments; i.e., strain amplitude, frequency, and temperature are held constant. Full frequency sweeps, $\omega = 10^{-3}-10^{2}$ rad/s, were selectively performed at small shear amplitude, $\gamma = 1\%$, to acquire a more complete rheological characterization. Some specimens were quenched (<1 min) to room temperature immediately after LAOS, while others were quiescently annealed in the rheometer at 150 °C. SEC tests performed before and after the rheological tests indicate that no substantial sample degradation occurred.

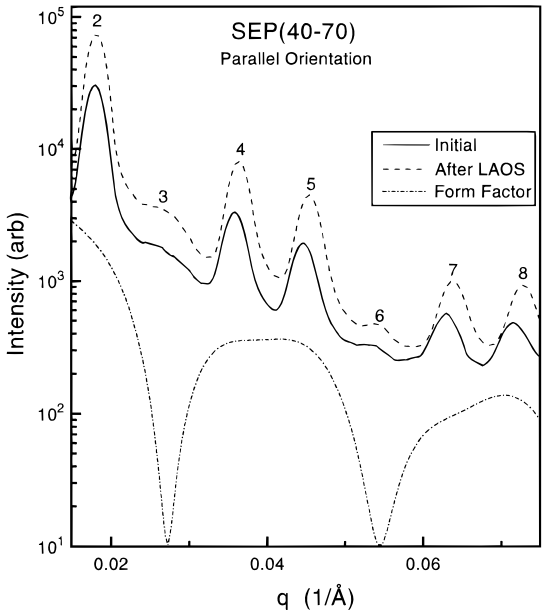

Figure 2. Small-angle X-ray scattering intensity versus scattering angle along the 2* direction, in the 1*−2* plane, for SEP(40−70) in the initial state (—) ($d = 715 \pm 3$ Å) and quenched after orientation (- - -) ($d = 690 \pm 3$ Å). The form factor for this structure ($\Phi_{PS} = 0.322$) is also shown (- · -).

SAXS. Small-angle X-ray scattering (SAXS) was performed on two instruments. Experiments at Princeton University employed Cu Kα ($\lambda = 1.54$ Å) radiation generated by a Rigaku RU-200BH rotating anode operated at 45 kV with a 0.2 × 2 mm microfocus cathode and Franks mirror optics. At the end of a 1.0 m evacuated flight path, two-dimensional images were collected with an image-intensified area detector[27] designed around a Thomson CCD chip. This beam line is equipped with an evacuated sample chamber and a pair of thermoelectric devices which maintained the sample at the temperature of interest during the *in situ* annealing studies. SAXS patterns were taken at room temperature except for the *in situ* annealing study, which was performed at 150 °C. SAXS at the University of Pennsylvania was performed using a reconditioned and upgraded Elliot GX-6 rotating anode (Cu Kα) operated at 40 kV with a 0.2 × 2 mm microfocus cathode, Franks mirror optics, and Ni foil monochromation. A Braun 1-D position-sensitive detector was used at the end of a 1.2 m He-filled flight path. Angular calibration of the detector was accomplished with a stained collagen sample from a duck's tendon which has a repeat distance of 609 Å and exhibits 10 orders of reflections. The measured scattered intensities were corrected for background scattering.

Scattering experiments were performed in the three principal directions relative to the parallel-plate geometry as shown in Figure 1. Because the three directions are mutually orthogonal, the reciprocal space directions are parallel to the real space directions. The reciprocal space directions are denoted by an asterisk (*) and correspond to the customary rheological notation: 1 direction, velocity direction; 2 direction, velocity gradient; and 3 direction, neutral direction. Samples were cut as necessary so that the path length through the sample was ∼1 mm.

III. Results

(a) SAXS. The initial state of the SEP(40−70) diblock copolymer is characterized in part by the scattering profile shown in Figure 2. A lamellar microstructure is indicated by the positioning of the Bragg

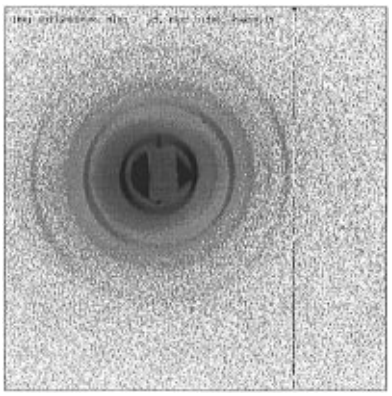

Figure 3. Representative two-dimensional SAXS pattern of the initial morphology of SEP(40−70). Note that the intensity scale for this and all subsequent 2-D SAXS patterns is nonlinear and based on a power law exponential.

peaks at integer multiples of the first-order peak. The reduced intensity of every third peak is due to the close proximity of a minimum in the form factor,[28,29] corresponding to a polystyrene volume fraction of, $\Phi_{PS} \cong {}^1/_3$. A representative 2-D SAXS pattern of the initial state of SEP(40−70) is displayed in Figure 3. While a weak ring of intensity is indicative of isotropic orientation, SEP(40−70) displays two broad maxima superimposed upon a weak ring, indicating that there is a slightly greater population of lamellae in the plane of the shearing surfaces; i.e., the initial state has a slight preference for the parallel orientation. This slight preferential alignment of the lamellae caused by the sample preparation cannot be removed by annealing in the disordered state because the MST of SEP(40−70) is not accessible. The pattern of Figure 3 is from a specimen which was removed from the rheometer after the *initial* rheological state was characterized. From this and comparable SAXS patterns taken of specimens as cast and as molded for the rheometer, we are confident that the sample preparation and handling do not cause the biaxial texture and lamellar thinning which we observe and attribute to LAOS.

A specimen quenched to room temperature immediately after cessation of 12 h of LAOS ($\gamma = 40\%$, $\omega = 1$ rad/s, 150 °C) is characterized by the three orthogonal scattering patterns in Figure 4a−c. After LAOS, the SAXS profiles show a greatly increased number of higher order reflections, especially along the 2* direction, indicating improved long-range order of the lamellae. Though not all visible in this print, at least 13 orders of reflections were detected in the 2* direction.

Examining the 1*−2* plane in Figure 4a reveals two sets of scattering maxima, indicating that a biaxial texture has been induced by the shearing. The scattering maxima along the 2* direction correspond to lamellae in the parallel orientation, while the second set of maxima close to the 1* direction correspond to lamellae in a nearly transverse orientation. This second orientation is noted as nearly transverse because these diffraction maxima and therefore the lamellae associated with them are inclined at ∼80° to the primary orientation. The higher intensities of the maxima along 2* imply that the biaxial texture contains predominantely the parallel orientation and that the nearly transverse orientation is a significantly smaller component.[30]

The SAXS patterns taken in the other two principal directions (Figure 4b,c) confirm the presence of the biaxial orientation. Of notable interest is the absence of any appreciable scattering along the 3* direction,

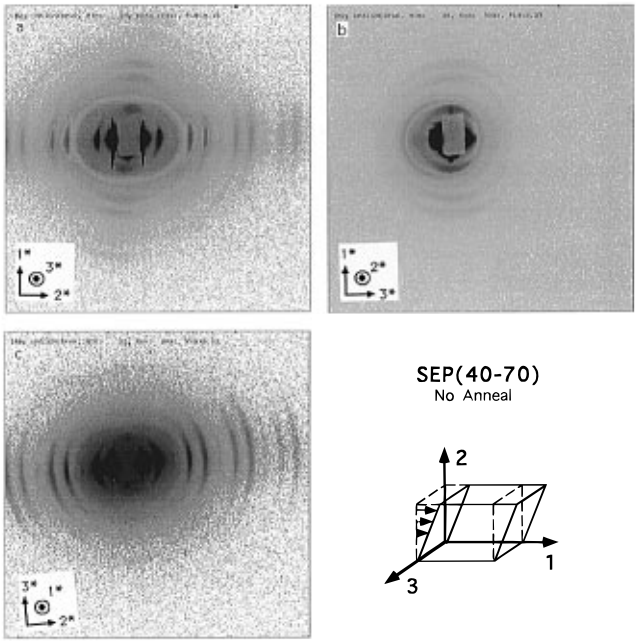

Figure 4. Orthogonal SAXS patterns for SEP(40−70) as quenched after 12 h of large-amplitude oscillatory shear (LAOS). Patterns correspond to the incident X-ray beam along the neutral (a), gradient (b), and velocity (c) directions.

Table 1. Azimuthal fwhm of the Fourth-Order Peaks Corresponding to the Parallel Orientation for SEP(40−70)

	1*−2* plane	2*−3* plane
LAOS and quenched	17°	23°
LAOS and 168 h anneal	29°	40°

which indicates a lack of lamellae oriented in the perpendicular orientation.

The large-amplitude oscillatory shearing also causes a decrease in the lamellar long period associated with the parallel orientation, i.e., a thinning of the parallel lamellae. Figure 2, displaying the q dependence of the peaks along the 2* direction, shows the peaks to be shifted to larger q values after LAOS. Samples quenched immediately following LAOS display a d spacing for the parallel orientation of 690 ± 3 Å, which is ∼4% smaller than the initial (and presumably equilibrium) spacing of 715 ± 3 Å. The transverse orientation does not undergo a similar thinning and retains the equilibrium d spacing of 715 ± 3 Å.

The extent of orientational order induced can be characterized by the azimuthal breadth of the scattered peaks. A more random orientation of lamellae about a given direction corresponds to an increased spatial distribution of scattering centers about that direction, creating a broader azimuthal scan. Azimuthal scans were radially integrated about the fourth-order scattering maxima of the parallel orientation then normalized to unit intensity and fit with a Gaussian to determine the full width at half-maximum (fwhm). Table 1 displays the azimuthal fwhm's obtained from the 1*−2* and 2*−3* planes of the SAXS patterns in Figure 4. The larger azimuthal breadth observed in the 2*−3* plane is consistent with the previous work of Winey et al.[7] for a low molecular weight SI diblock. It indicates that there is a broader distribution of lamellar normals about the velocity axis than the neutral axis and supports the theoretical prediction of shear-induced undulational instabilities.[13,25,31]

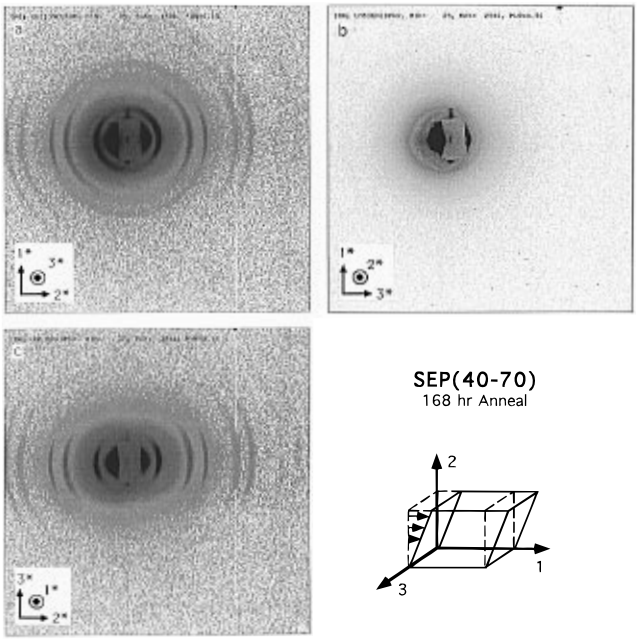

Figure 5. Orthogonal SAXS patterns for SEP(40−70) which has been subjected to LAOS, annealed for 168 h at 150 °C, and cooled to room temperature. Patterns correspond to the incident X-ray beam along the neutral (a), gradient (b), and velocity (c) directions.

Annealing the specimens after LAOS significantly alters the morphology. Figure 5 displays the three orthogonal scattering patterns of a sample which was subjected to LAOS, quenched, and then quiescently annealed in a vacuum oven for 168 h at 150 °C. The disappearance of the second set of scattering maxima in the 1* direction, as observed in both the 1*−2* and 1*−3* planes, indicates that annealing destroys the biaxial texture by eliminating the nearly transverse orientation. Examining the scattering pattern in the 1*−2* plane more closely reveals that the uniaxial pattern due to the parallel orientation is superimposed upon a weak ring of intensity.

These morphology changes upon annealing were further investigated by studying a specimen which, after being subjected to LAOS, was quenched, removed from the rheometer, and subsequently annealed *in situ* in the SAXS apparatus at 150 °C. Figure 6a depicts the intensity distribution of the second-order peaks in the 1*−2* plane as a function of the azimuthal angle at various anneal times. The increase in scattered intensity observed at $\mu \approx 45°$ is due to the buildup of a weak ring of scattered intensity, while the decrease in intensity of the peak at $\mu \approx 80°$ is due to the disappearance of the nearly transverse orientation. Although a significant fraction of the lamellae retain the original orientations as evidenced by the intensity of the maxima at $\mu = 0°$, the increase in the azimuthal fwhm with annealing, Figure 6b, reveals a decrease in the extent of alignment of the parallel orientation. Thus, the global alignment of the specimen is becoming less perfect, not more, with annealing.

Upon annealing, the radial width of the peaks decreases, indicating an increase in the degree of long-range order in the material. The peaks also shift to smaller q values corresponding to an increase in the lamellar thickness. For the sample which was quenched immediately following LAOS and subsequently annealed in the SAXS apparatus, Figure 7 shows the lamellar spacing of the parallel orientation regaining its initial value upon annealing. In contrast, the lamellae in the nearly transverse orientation maintain the same d spacing (~715 Å), before and after LAOS.

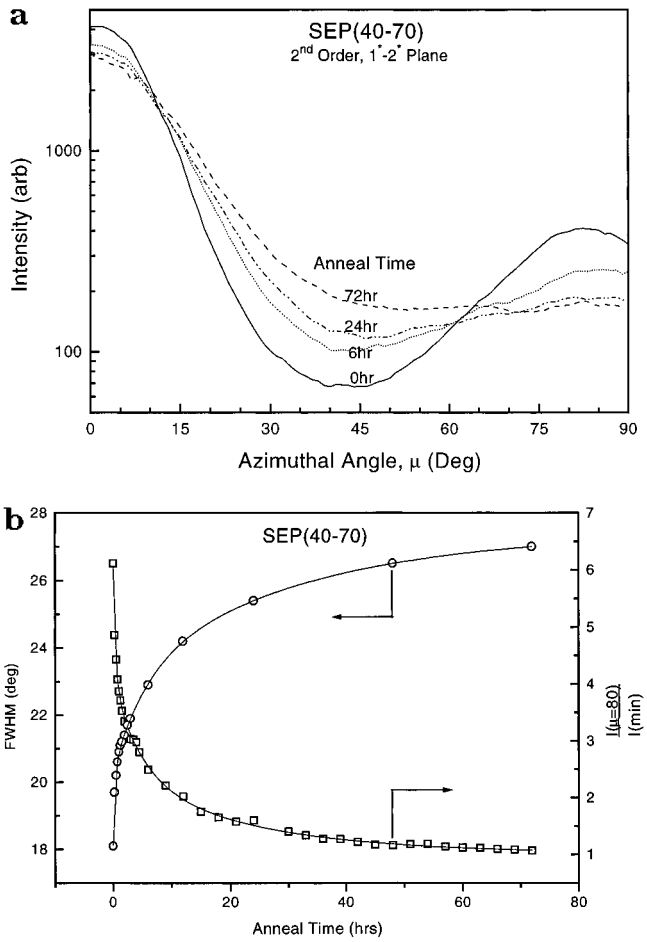

Figure 6. (a) Scattered intensity of the second-order diffraction maxima as a function of azimuthal angle as observed in the 1*−2* plane. The SEP(40−70) specimen was subjected to LAOS, quenched, and subsequently annealed *in situ* at 150 °C in the SAXS apparatus. (b) Azimuthal full width at half-maximum for the second-order reflection centered at $\mu \approx 0°$ (○) and the ratio of the maximum intensity at $\mu \approx 80°$ to the minimum azimuthal intensity (□), both as functions of the *in situ* anneal time. The solid lines in (b) represent fits to multiple exponential decay functions.

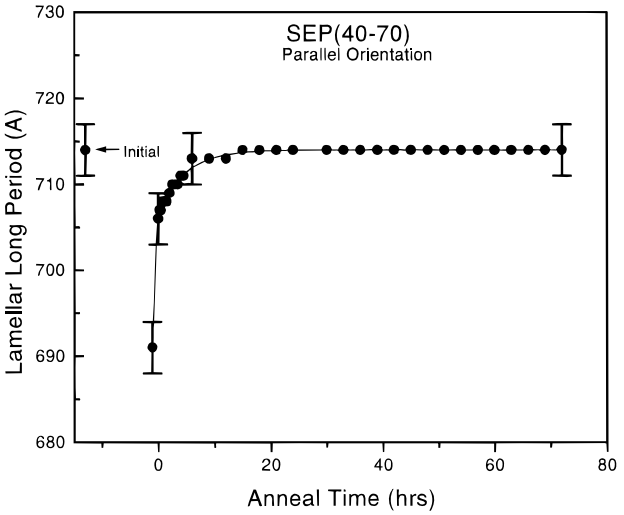

Figure 7. Long period of the lamellae in the parallel orientation as a function of *in situ* anneal time at 150 °C for the specimen studied in Figure 6. The solid line is a fit to a multiple exponential decay function.

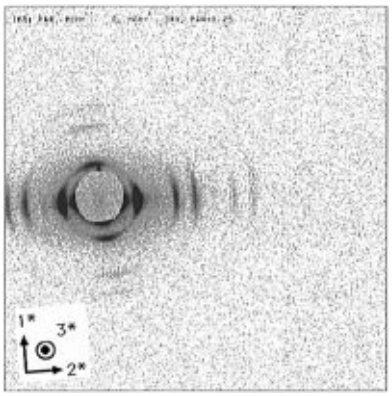

Figure 8. SAXS pattern of an SEP(40−70) specimen which was oriented through LAOS for 12 h followed by 168 h of annealing at 150 °C and then subjected to a second application of LAOS followed immediately by quenching. This pattern corresponds to the incident X-ray beam along the neutral direction, (1*−2* plane).

After relaxation of the shear-induced orientations through prolonged annealing, a second application of LAOS restores the biaxial texture. Figure 8, displays the 1*−2* SAXS pattern for a specimen which was oriented through LAOS for 12 h followed by 168 h of annealing at 150 °C and then subjected to a second application of LAOS followed immediately by quenching. The parallel orientation again dominates the pattern with the nearly transverse orientation inclined at ∼80°. The lamellar contraction reported above is also observed: parallel ∼690 Å, nearly transverse ∼715 Å.

(b) Rheology. Figure 9a displays the dynamic mechanical response of the initial state of SEP(40−70), corresponding to the morphology shown in Figure 3, i.e., before the application of large-amplitude oscillatory shear. The slope of the dynamic moduli at low frequencies is indicative of the microphase-separated state.[20,32,33] At all frequencies, the dynamic storage modulus, G', is greater than the dynamic loss modulus, G''. Figure 10 shows the effective dynamic storage and loss moduli during the application of the *orientation* shear. The moduli decrease with the application of the large-amplitude shear. This drop occurs rapidly at first and then continues, although more gradually, throughout the duration of the LAOS, with a greater percentage decrease occurring in G' than in G''. This behavior of the moduli during LAOS concurs with previous studies on lamellar diblock copolymers of various molecular weights and compositions.[7,8]

After 12 h, the large-amplitude orientation shearing ceased and the recovery of the rheological response was tracked using the probe condition to periodically measure the moduli as the sample was annealed in the rheometer (Figure 11). The moduli recover rapidly at first, followed by a much more gradual recovery, but do not approach their initial values during the lifetime of this experiment (∼48 h). Other samples were annealed for up to 7 days and show equivalent trends. If the rate of recovery is assumed to be constant at long anneal times, >48 h, then extrapolation of the data reveals that ∼25 years would be required for the moduli to recover fully under these conditions.

The rheological response is changing so slowly after 48 h of annealing that for our purposes we consider this the final state for comparison with the sample before LAOS. Figure 9a shows the frequency dependence of G' and G'' before LAOS and after LAOS with a subsequent 48 h anneal. We refer to these two states simply

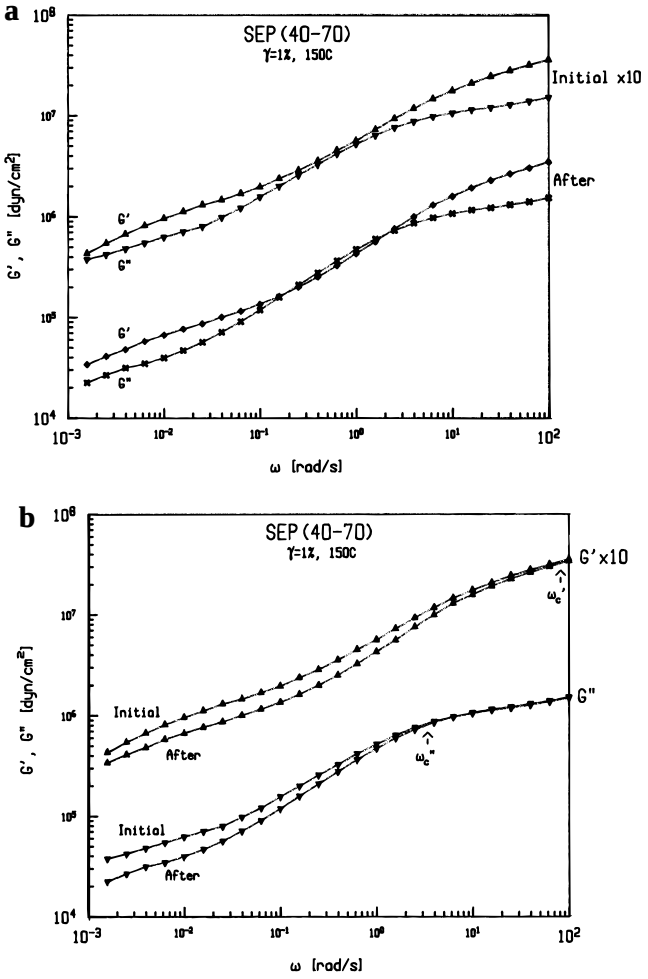

Figure 9. Frequency dependence of the dynamic storage (G') and loss (G'') moduli at 150 °C for SEP(40−70) before (initial) and after subjection to the strong shearing: (a) displays the initial data shifted vertically; (b) displays the G' data shifted vertically.

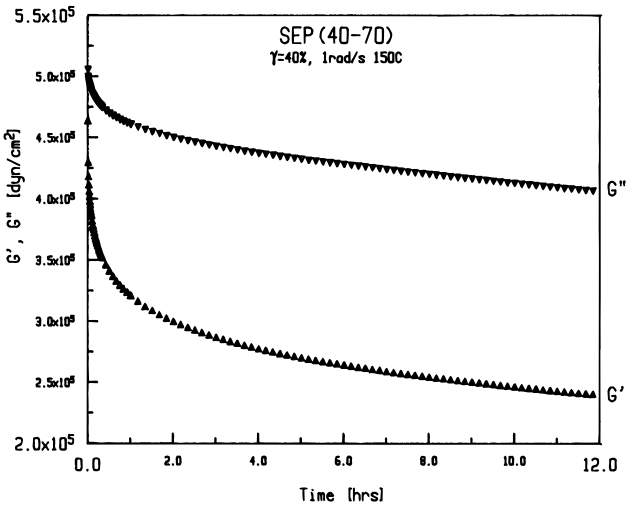

Figure 10. Effective dynamic storage (G') and loss (G'') moduli as functions of time during LAOS: T = 150 °C, γ = 40%, ω = 1 rad/s.

as "initial" and "final" and have shifted the initial data vertically for clarity. It is evident that the nature of the response has been significantly altered by the application of the *orientation* shear. Two notable changes are in the region of intermediate frequency where after

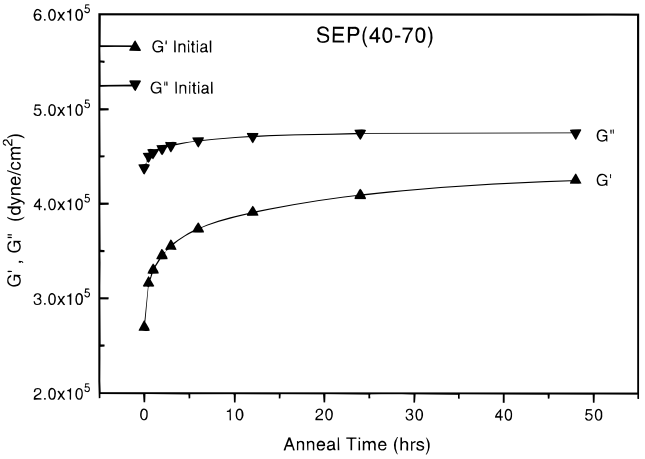

Figure 11. Dynamic storage (G') and loss (G'') moduli, measured intermittently ($\omega = 1$ rad/s, $\gamma = 1\%$), as functions of time during post-orientation annealing at 150 °C. The moduli prior to orientation are shown (initial). The solid line is a fit to a multiple exponential decay function.

LAOS G'' has become greater than G', creating a double crossover, and in the region of low frequency where after LAOS the slopes of G' and G'' are approximately equal.

The net effect of the strong shearing is to create a final state which has a lower modulus. This is more readily seen in Figure 9b, which displays the G' data shifted vertically for clarity. The data display branch points, ω_c' and ω_c'', between the initial and final states at frequencies below which the molecular response has been permanently altered by the strong shearing. Other researchers have observed similar branch points in data taken above and below the MST in which the molecular response is altered by the creation of the microdomains. As mentioned earlier, this material does not have an accessible MST. We are therefore not able to determine if the branch points between the homogeneous and the isotropic microphase-separated states occur at the same frequencies as those we observe between our initial "isotropic" and final "aligned" states. However, our results are consistent with earlier work[5,9,17,34] which show that the branch point for G', ~100 rad/s, occurs at a frequency at least an order of magnitude higher than for G'', ~2.5 rad/s. Thus, the local order of the microdomains and the global orientational order influence the linear elastic response over a wider frequency range and up to higher frequencies than the linear viscous response.

(c) Blends. Blends containing 5% or 10% S(30) qualitatively exhibit the same rheological response as described above for the neat SEP(40−70) before, during, and after LAOS. As we have demonstrated, the rheological response is significantly affected by the global state of orientation. Our inability to produce an equivalent, isotropic, starting state for all samples hinders our ability to quantify the exact changes which are taking place with the addition of the homopolymer upon strong shearing.

The SAXS results for the 5% and 10% blends are very similar to the neat system and display the same trends as described above. For this reason, we include only one set of representative scattering patterns in Figure 12 which show the shear-induced biaxial texture. With regard to the lamellar contraction, while the addition of homopolymer increases the equilibrium spacing of the lamellae, the relative contraction due to shearing remains at ~4%.

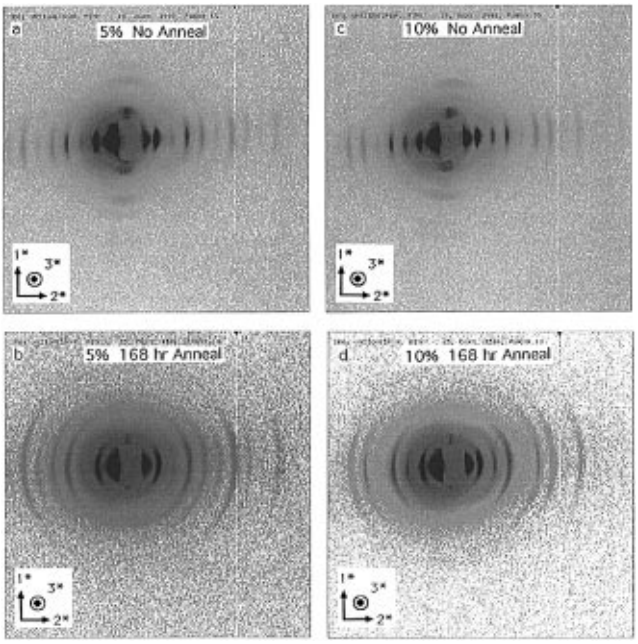

Figure 12. SAXS patterns for SEP(40−70)/S(30) 5% and SEP-(40−70)/S(30) 10% blends subjected to LAOS and then quenched, (a) and (c) respectively, and quenched and subsequently annealed at 150 °C for 168 h, (b) and (d) respectively. Patterns correspond to the incident X-ray beam along the neutral direction.

An interesting observation in the blend specimens is that the homopolymer remains in the microdomains and is not driven out by the strong shearing, alignment, and thinning processes. In the neat system, the form factor corresponding to the polystyrene volume fraction, $\Phi_{PS} = 0.327$, diminishes every third scattering peak as shown in Figure 2. The addition of the homopolystyrene swells the styrene lamellae, increasing Φ_{PS} to 0.383, which changes the form factor to one which only partially diminishes the third-order peak and greatly reduces the fifth- and eighth-order peaks as shown in Figure 13. After LAOS, the relative intensities of the observed diffraction peaks for the blend remain unchanged, indicating that the homopolystyrene remains in the polystyrene block microdomains.

IV. Discussion

The SAXS patterns of the 1*−2* plane demonstrate that our large-amplitude oscillatory shearing condition induces a biaxial lamellar texture not only in the neat system, similar to that found by Okamoto et al.,[26] but also in the blends. The 1*−2* pattern is also our strongest evidence for the coexistence of two different lamellae spacings. From this single scattering pattern we are able to measure a distinct d spacing for each of the two lamellae orientations, greatly diminishing the possibility that the difference measured is due to experimental error. Further evidence for our reported thinning of the lamellae in the parallel orientation is the recovery of the lamellae spacing during the *in situ* annealing SAXS experiment.

It seems appropriate to question why the contraction of block copolymer lamellae has not been previously reported. Two elements are necessary to detect this phenomenon: sufficient experimental resolution and a sufficiently slow recovery time of the lamellar thickness. The use of an electronic detector rather than X-ray film and a long flight path combine to provide the necessary resolution in reciprocal space. Presently, the param-

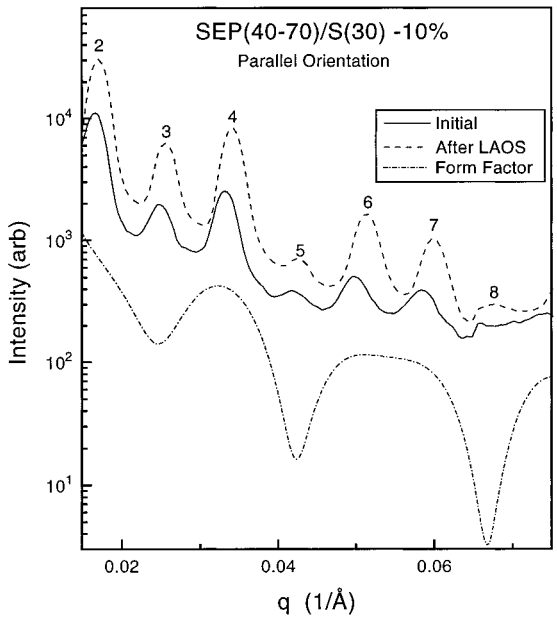

Figure 13. SAXS intensity versus scattering angle along the 2* direction, in the 1*−2* plane, for SEP(40−70)/S(30) 10% in the initial state (—) ($d = 755 \pm 3$ Å) and as quenched after LAOS (- - -) ($d = 725 \pm 3$ Å). The form factor for this structure ($\Phi_{PS} = 0.383$) is also shown (- · -).

eters which govern the recovery time of the lamellae spacing are speculative but probably include the extent of entanglement in the block copolymer, the proximity to the glass transitions and the MST, and possibly the presence of the biaxial texture. As the recent paper of Okamoto et al.[26] does not report the lamellae spacing as a function of shearing or annealing, it is unclear whether they detected a lamellar contraction.

Lamellar contraction has recently been predicted by Williams and MacKintosh using a free energy expression to describe the effect of oscillatory shear in the strong segregation limit.[25] They consider only the parallel orientation of symmetric diblocks in the melt and offer the following argument: "Shear tilts each chain and stretches it more than in an un-sheared lamellae. To avoid this penalty, the lamellar spacing should decrease."[25] Their derivation predicts a spacing change, Δd_{min}, relative to the unperturbed spacing, d_0, which can be estimated by $\Delta d_{min}/d_0 = -\sigma^2/(\sigma^2 + 3M^2)$, in which σ is the applied shear stress at the surfaces and M is the modulus of the lamellae. For the strong oscillatory shearing of our experiments, the theory predicts a contraction of the lamellar spacing of ∼5%, which is surprisingly close to our experimentally observed ∼4% contraction. Considering the theoretical assumptions and our approximations used to obtain a tractable result, it is encouraging that the theory predicts a value in the same order of magnitude as our experimental results. Additional experiments are certainly required to thoroughly analyze the validity of the theory.

A notable discrepancy, namely the angle between the parallel and the transverse orientations, exists between the biaxial texture that Okamoto et al. report[26] and that which we observe. The block copolymers and shearing conditions used in the two studies are comparable. Their 2D SAXS patterns appear to exhibit a 90° angle between the two coexisting orientations, while our data show a nearly transverse orientation inclined at ∼80° relative to the parallel orientation. This 80° angle, which has been reproduced in every sample, implies that a symmetry-breaking event has occurred. We offer a tentative explanation for this difference. After LAOS, both the sample and the stainless steel sample fixtures cool to room temperature in the rheometer. Upon cooling, the thermal contraction of the fixtures could apply a shear stress on the sample in the direction of the applied shear. It is this final "half cycle" of shear which causes the transverse orientation to be preferentially inclined at ∼80° (in only one direction). By assuming a simple axial thermal gradient along the sample tools, the thermal contraction is calculated to be 0.2−0.3 mm (corresponding to a 20−30% strain amplitude) creating an angle of 78°−82°, which is in agreement with the angle of inclination we observe. In contrast, the experiments of Okamoto et al. were performed *in situ*, so that no tilting of the transverse orientation should occur. The geometry of the fixtures is such that thermal contraction does not significantly alter the sample thickness, and therefore it cannot be used to explain the lamellar thinning which we report.

Previous researchers have proposed mechanisms of macroscopic alignment based on results of alignment occurring during strong shearing. We have shown that changes in macroscopic alignment can occur not only during the application of strong shearing but also during subsequent quiescent annealing. In order to contribute to the ongoing discussion about the mechanism of alignment, we turn our attention to the transformation of the morphology upon annealing and attempt to correlate it to the recovery of the rheological response.

The transformation of the morphology of SEP(40−70) upon annealing was characterized by three parameters: the relaxation of the parallel orientation, given by the increase of the fwhm of the azimuthal scattering intensity of the parallel orientation, Figure 6b; the disappearance of the transverse orientation, given by the ratio of the maximum intensity for the transverse peak, $I(m\sim80°)$, to the minimum intensity, $I(\text{min})$, attributed to the isotropic ring, Figure 6b; and the regrowth of the lamellar thickness, Figure 7. These parameters as well as the recovery of the dynamic moduli are well represented by multiple exponential decay functions of the form $G = A + B\exp(t/\tau_1) + C\exp(t/\tau_2)$. It should be emphasized that because more than one time constant is required, more than one relaxation mechanism is probably involved. The initial time constant for the relaxation of the parallel orientation, $\tau_1 \approx 0.33$ h, is consistent with that found by Okamoto et al.,[26] and is similar to those for the fading of the transverse orientation, $\tau_1 \approx 0.35$ h, and the regrowth of the lamellar thickness, $\tau_1 \approx 0.25$ h. The relaxation time observed for the recovery of the modulus of SEP(40−70), $\tau_1 \approx 0.3$ h, is comparable to the relaxation times corresponding to the morphological changes. This suggests that the relaxation and reorientation of the lamellar morphology is the basis for the recovery of the moduli. In contrast, other researchers[4] have suggested that the re-formation of block copolymer microdomains across the grain boundaries causes the moduli recovery. The disparity between these ideas is significant in the context of the mechanisms of macroscopic orientation.

There are presently two hypotheses regarding the mechanism of macroscopic alignment of block copolymer microdomains: grain destruction with re-formation,[2,6,35,36] and grain rotation.[2,4,8,35] In addition, an alignment mechanism which maintains lamellar continuity across the block copolymer grain boundaries should be consid-

ered. Tilt and twist grain boundaries which have continuous, microphase-separated, microdomains have been reported by Gido et al.[37] for a lamellar diblock copolymer in the absence of shear. We suggest that alignment could occur via the movement of these boundaries by locally untwisting and/or unbending, so as to allow the growth of one grain at the expense of another while maintaining the lamellar morphology.

Our preliminary support for this comes from the disappearance of the transverse orientation with annealing, and its subsequent return upon reshearing. Recall that a narrower spatial distribution of lamellae was observed in the 1*−2* plane. It is therefore likely that the transverse orientation represents a local energy minimum under our shearing conditions. Combining this with the suspected global minimum of the parallel orientation, we conclude that LAOS creates a shear-stabilized morphology, namely the biaxial texture observed. This morphology becomes unstable during quiescent annealing following the cessation of LAOS. The observed destruction of the nearly transverse orientation occurs by the random repositioning of the transverse lamellae away from their shear-stabilized orientation. The scattering associated with the transverse orientation was shown to fade into an isotropic ring in the 1*−2* plane while it vanished in the 1*−3* plane, implying that these transverse lamellae are reorienting in the 1*−2* plane, with their normals remaining essentially perpendicular to the neutral axis. A relatively slight unbending of the grain boundaries between the parallel and transverse orientations to relieve the residual stresses induced by the shearing would account for this. The second application of the LAOS merely realigns the transverse lamellae back into their preferred orientation for the given applied stress field. A better understanding of the nature of the nearly transverse orientation, the mechanism through which it disappears, and of the size scales on which it occurs is currently being studied via electron microscopy.

Acknowledgment. Work at the University of Pennsylvania was supported by NSF−IMR (93-05286), NSF−MRL (91-20668), and the University Research Foundation. B.S.P. is grateful for support from an Ashdon Fellowship, and K.I.W. for support from NSF−YIA (94-57997). Work at Princeton University was supported by the U.S. DOE (DE-FG02-87ER60522) and NSF−DMR (92-23966).

Supporting Information Available: Complete equations for the multiple exponential decay curve fitting of the data (1 page) and calculations for the theoretical lamellar contraction (1 page). Ordering information is given on any current masthead page.

References and Notes

(1) Folkes, M. J.; Keller, A.; Scalisi, F. P. *Colloid Polym. Sci.* **1973**, *251*, 1.
(2) Hadziioannou, G.; Mathis, A.; Skoulis, A. *Colloid Polym. Sci.* **1979**, *257*, 15.
(3) Annighofer, F.; Gronski, W. *Makromol. Chem., Rapid Commun.* **1983**, *4*, 123.
(4) Morrison, F.; Bourvellec, G. L.; Winter, H. H. *J. Appl. Polym. Sci.* **1987**, *33*, 1585.
(5) Koppi, K. A.; Tirrell, M.; Bates, F. S.; Almdal, K.; Colby, R. H. *J. Phys. II Fr.* **1992**, *2*, 1941.
(6) Scott, D. B.; Waddon, A. J.; Lin, Y.-G.; Karasz, F. E.; Winter, H. H. *Macromolecules* **1992**, *25*, 4175.
(7) Winey, K. I.; Patel, S. S.; Larson, R. G.; Watanabe, H. *Macromolecules* **1993**, *26*, 2542.
(8) Kannan, R. M.; Kornfield, J. A. *Macromolecules* **1994**, *27*, 1177.
(9) Patel, S. S.; Larson, R. G.; Winey, K. I.; Watanabe, H. *Macromolecules* **1995**, *28*, 4313.
(10) Albalak, R. J.; Thomas, E. L. *J. Polym. Sci., B: Polym. Phys.* **1994**, *32*, 341.
(11) Cates, M. E.; Milner, S. T. *Phys. Rev. Lett.* **1989**, *62*, 1856.
(12) Fredrickson, G. H. *J. Rheol.* **1994**, *38*, 1045.
(13) Goulian, M.; Milner, S. T. *Phys. Rev. Lett.* **1995**, *74*, 1775.
(14) Gupta, V. K.; Krishnamoorti, R.; Kornfield, J. A. *Macromolecules* **1995**, *28*, 4464.
(15) Kornfield, J. A.; Kannan, R. M.; Smith, S. *Polym. Prepr. (Am. Chem. Soc., Div. Polym. Chem.)* **1994**, *34*, 676.
(16) Bates, F. S.; Bair, H. E.; Hartney, M. A. *Macromolecules* **1984**, *17*, 1987.
(17) Rosedale, J. H.; Bates, F. S. *Macromolecules* **1990**, *23*, 2329.
(18) Winey, K. I.; Patel, S. S.; Larson, R. G.; Watanabe, H. *Macromolecules* **1993**, *26*, 4373.
(19) Morrison, F. A.; Mays, J. W.; Muthukumar, M.; Nakatani, A. I.; Han, C. C. *Macromolecules* **1993**, *26*, 5271.
(20) Larson, R. G.; Winey, K. I.; Patel, S. S.; Watanabe, H.; Bruinsma, R. *Rheol. Acta* **1993**, *32*, 245.
(21) Winey, K. I.; Thomas, E. L.; Fetters, L. J. *Macromolecules* **1992**, *25*, 2645.
(22) Winey, K. I.; Thomas, E. L.; Fetters, L. J. *J. Chem. Phys.* **1991**, *95*, 9367.
(23) Hashimoto, T.; Tanaka, H.; Hasegawa, H. *Macromolecules* **1990**, *23*, 4378.
(24) Pinheiro, B. S.; Winey, K. I. *Polym. Prepr. (Am. Chem. Soc., Div. Polym. Chem.* **1995**, *36*, 174.
(25) Williams, D. R. M.; MacKintosh, F. C. *Macromolecules* **1994**, *27*, 7677.
(26) Okamoto, S.; Saijo, K.; Hashimoto, T. *Macromolecules* **1994**, *27*, 5547.
(27) Tate, M. W.; Eikenberry, E. F.; Gruner, S. M. In preparation.
(28) Guinier, A.; Fournet, G. *Small Angle Scattering of X-Rays*; Wiley: New York, 1955.
(29) *Small Angle X-ray Scattering*; Glatter, O., Kratky, O., Eds.; Academic Press: New York, 1982.
(30) Weissenberg, K. *Z. Phys.* **1961**, *8*, 20.
(31) Bruinsma, R.; Rabin, Y. *Phys. Rev. A* **1992**, *45*, 994.
(32) Kawasaki, K.; Onuki, A. *Phys. Rev. A* **1990**, *42*, 3664.
(33) Bates, F. S. *Macromolecules* **1984**, *17*, 2607.
(34) Winey, K. I.; Gobran, D. A.; Xu, Z.; Fetters, L. J.; Thomas, E. L. *Macromolecules* **1994**, *27*, 3520.
(35) Morrison, F. A.; Winter, H. H. *Macromolecules* **1989**, *22*, 3533.
(36) Scott, D. B. Ph.D. Thesis, University of Massachusetts, 1992.
(37) Gido, S. P.; Gunther, J.; Thomas, E. I.; Hoffman, D. *Macromolecules* **1993**, *26*, 4506.

MA951284O